Photodoping and Enhanced Visible Light Absorption in Single-Walled Carbon Nanotubes Functionalized with a Wide Band Gap Oligomer

Benjamin R. Bunes, Miao Xu, Yaqiong Zhang, Dustin E. Gross, Avishek Saha, Daniel L. Jacobs, Xiaomei Yang, Jeffrey S. Moore, and Ling Zang**

Owing to their desirable electronic properties,[1] carbon nanotubes (CNTs) have garnered significant attention, most notably in optoelectronic applications. Indeed, CNTs have been used in photovoltaic cells,[2] photodetectors,[3] and light-emitting diodes.[4] However, their use has been limited to the laboratory scale for a number of reasons, including difficulty in device fabrication due to insolubility and narrow absorption bands arising from the shape of the density of states.[5] In this paper, a means to improve solubility while broadening the absorption bands is presented. The broadband enhancement is achieved through the formation of a charge transfer complex between the CNT and a wide band gap oligomer. This interaction may provide the basis for achieving practical broadband optoelectronic devices using CNTs.

Solubility can be substantially improved through chemical modification, both covalent and noncovalent. Covalent methods are robust, but will change the electronic properties of the CNT,[6] except in very specific cases.[7] Noncovalent methods provide a wide range of materials that can be used without changing the band structure of the CNT.[8] Indeed, this strategy has been shown to improve dispersion in solution,[9] increase uniformity on a substrate,[10] isolate single species from mixtures of different CNT configurations,[11] and enhance selectivity in chemical sensor applications.[12] Furthermore, the functional materials can also form donor/acceptor pairs with the CNT, providing additional effects under light exposure,[13] as shown in our previous work.[14]

While the optoelectronic characteristics of other 1D materials have attracted interest,[15] CNTs are unique in their large area of π-conjugation, which provides opportunities for surface modification through donor and acceptor π–π interactions.[16] This relatively strong interaction enables additional effects, such as the formation of charge transfer complexes.[17] While there are a few reports of charge transfer complexes formed between organic molecules and CNTs using optical measurements,[18] no such reports were found on the impact of complexation on optoelectronic behavior. Further study is required to understand the nature of these donor–acceptor interactions so that materials can be designed to optimize the performance of optoelectronic devices featuring CNTs.

Herein, a carbazolylethynylene oligomer (namely Tg-Car, **Figure 1**a) is used to disperse semiconducting single-walled CNTs in chloroform. Materials based on carbazole[19] and similar structures[20] have been used extensively to suspend CNTs. Films cast from the dispersion were free from aggregation, which is crucial for device repeatability and uniformity. While the energy levels of the oligomer suggest it should be an electron donor and absorb ultraviolet light,[21] field effect transistors fabricated from the CNTs with surface-adsorbed oligomer show that it is an electron acceptor when exposed to visible light. The direction of the electron transfer is observed by a positive shift in threshold voltage, indicating an increased hole concentration within the CNT. This effect is accompanied by enhanced absorption in the visible spectrum attributed to the formation of a charge transfer complex. This work may provide design criteria to expand the absorption spectra and enhance charge separation, leading to improved solar cells and photodetectors.

CNTs were dispersed in chloroform using a process previously developed in our lab.[14] The single-walled CNTs used in this report are mainly semiconducting (>90%). Tg-Car oligomers were employed; on average, each oligomer contained 19 repeat units. The synthesis of this oligomer is described elsewhere.[22] Briefly, CNTs were placed in chloroform with excess Tg-Car and sonicated for 90 min (Figure 1a). Aggregates were removed through centrifugation (see the Experimental Section for details). The result was CNTs suspended in chloroform with Tg-Car adsorbed (Figure 1b). The energy levels of the highest occupied molecular orbital (HOMO) and lowest unoccupied molecular orbital (LUMO) for the Tg-Car were calculated using

B. R. Bunes, Dr. M. Xu, Y. Zhang, D. L. Jacobs, Dr. X. Yang, Prof. L. Zang
Nano Institute of Utah and Department of Materials Science and Engineering
University of Utah
Salt Lake City, Utah 84112, USA
E-mail: lzang@eng.utah.edu
Dr. D. E. Gross[+]
Department of Chemistry
University of Illinois at Urbana-Champaign
Urbana, Illinois 61801, USA
Dr. A. Saha[†]
Smalley Institute for Nanoscale Science and Technology and Department of Chemistry
Rice University
Houston, Texas 77005, USA
Prof. J. S. Moore
Departments of Chemistry and Materials Science and Engineering
University of Illinois at Urbana, Champaign
Urbana, Illinois 61801, USA
E-mail: jsmoore@illinois.edu
[+]Present address: Department of Chemistry, Sam Houston State University, Huntsville, Texas 77340, USA
[†]Present address: Department of Physical Chemistry, University of Erlangen-Nuremberg, 91058 Erlangen, Germany

DOI: 10.1002/adma.201404112

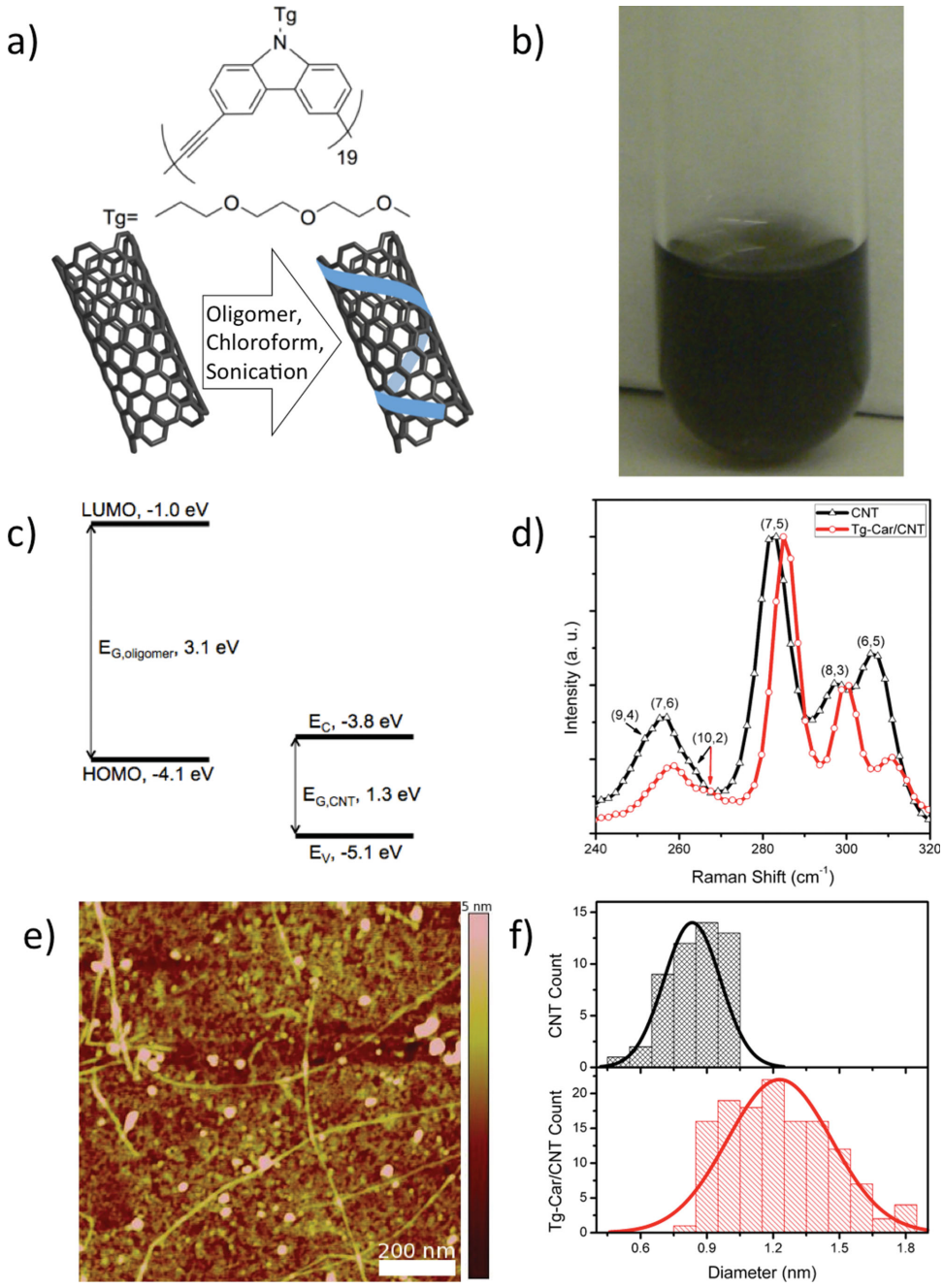

Figure 1. a) Molecular structure of the Tg-Car oligomer and schematic of the functionalization process. b) Photograph of the Tg-Car/CNT solution. c) Energy bands referenced to the vacuum level. Values for the oligomer were obtained from density functional theory calculation and those for the CNT are from the literature. d) Raman spectra of the pristine CNTs and Tg-Car/CNT. e) AFM image of Tg-Car/CNT on a silicon substrate. The material is free from aggregation. f) Histogram of CNT diameters extracted from AFM height measurements with and without Tg-Car. The presence of Tg-Car on the CNT surface is observed as a 50% increase in diameter.

the Gaussian 09 package with density functional theory and the values for the conduction and valance bands of the CNT are published elsewhere (Figure 1d).[23]

The presence of Tg-Car on the CNT surface is confirmed by Raman spectroscopy. Interaction with the Tg-Car causes the radial breathing mode associated with (7,5) CNTs to shift from 283.2 cm^{-1} to 285.8 cm^{-1} (Figure 1d). This demonstrates surface interaction between the Tg-Car and the CNT. Further analysis of the Raman data is presented in the Supporting Information (Figure S1, Supporting Information). The Tg-Car/CNT interaction is further confirmed through atomic force microscopy (AFM). Functionalized nanotubes showed good dispersion on the silicon dioxide (SiO_2) surface, with no aggregation observed (Figure 1e). The diameter of the Tg-Car/CNTs was measured from the height profile to be 1.2 ± 0.2 nm. This is significantly larger than the diameter of bare CNTs of

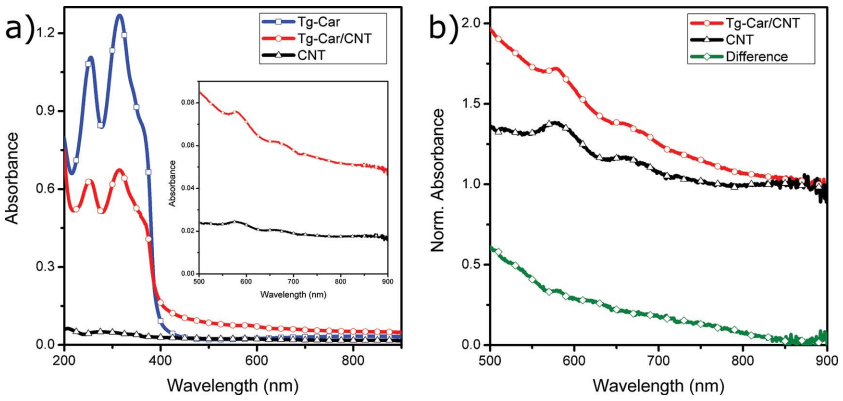

Figure 2. a) Absorption spectra for the carbon nanotube, Tg-Car oligomer, and Tg-Car/CNT composite. The inset displays an enlarged view of the enhanced region. b) The absorption spectra for the CNT and Tg-Car/CNT are normalized at 900 nm, which is attributed to only the CNT, to eliminate the effect of variation between the samples. The difference is also plotted, demonstrating improved absorption in the visible range despite the oligomer's wide band gap.

0.8 ± 0.1 nm (Figure 1f) measured by AFM under the same conditions. The measured size of bare CNTs is consistent with the manufacturer's specification. These measurements confirm the presence of the oligomer on the CNT surface. Further proof is provided by adhesion force microscopy measurements (Figure S2, Supporting Information).

Solid-state absorption spectra were obtained for Tg-Car, Tg-Car/CNTs, and bare CNTs (**Figure 2**a). The oligomer showed negligible absorption (attributed to scattering effects) at wavelengths longer than 400 nm. The pristine CNT film showed little absorption within the full range of the spectrometer. While the oligomer dominated the absorption spectrum of the Tg-Car/CNTs, an increase emerged in the visible region. Normalizing the spectra to the absorption at 900 nm (CNT only absorption) to account for the variation in concentration between the Tg-Car/CNT and bare CNT samples more clearly shows the enhanced absorption in the visible region (Figure 2b). The enhanced absorption applies to light with wavelengths less than 847 ± 27 nm. This enhanced absorption is attributed to the formation of a charge transfer complex between the CNT and Tg-Car oligomer.

Field effect transistors (FETs) were fabricated using the Tg-Car/CNTs. With a gap length of 5 μm and the average CNT length of 800 nm, it is clear that the devices use a network of Tg-Car/CNTs. The transfer characteristics show a low on current, which we attribute to the junctions between CNTs. The Tg-Car oligomer is insulating and occupies space between nanotubes at their junctions. Using the network has the benefit of mitigating the effects of the presence of metallic CNTs. Although the CNTs were purified by the manufacturer, a small amount of metallic CNTs is present. Because of their low concentration, the network prevents metallic CNTs from completely bridging the electrode gap. Therefore, removal of the metallic CNTs is not required. Upon illumination with a tungsten lamp, the threshold voltage shifted 4.2 ± 0.4 V from its original position in darkness (**Figure 3**a). This is in contrast to pristine nanotubes, which showed no photoresponse (Figure 3b). Shifting toward a more positive threshold indicates an increase in hole concentration within the CNT (p-type doping),[24] which contradicts the assumption that the oligomer is an electron donor (suggested by its small LUMO energy). Notably, the white light from a tungsten lamp contains few photons capable of exciting the oligomer (absorbing only wavelengths below 400 nm). A photoresponse at visible wavelengths is surprising and must arise from the enhanced absorption observed in the spectra in Figure 2b. Data regarding hysteresis and device properties (e.g., mobility) are presented in the Supporting Information (Figures S5 and S6, Supporting Information).

To gain insight into the mechanism of the doping, different long-pass filters were employed to restrict parts of the spectrum while keeping the flux of photons with energies exceeding that of the CNT's band gap (1.3 eV)[25] constant at 3×10^{16} photons cm^{-2} s^{-1}. Wavelength-dependent behavior was obtained in this manner (Figure 3c,d). The threshold shift persisted until wavelengths below 495 nm were removed and decreased thereafter. Projecting to zero threshold shift suggests no photoresponse to wavelengths longer than 833 ± 37 nm (or less than ≈1.5 eV), which corresponds to neither the CNT's band gap (1.3 eV) nor that of the oligomer (3.1 eV). This does, however, correlate to the charge transfer complex observed in the absorption spectral measurement (Figure 2b).

Holding constant the flux of photons whose energies exceed the CNT's band gap proves the photoresponse is not due to excitation in the CNT alone (otherwise, the response would be constant across the spectrum used). By calculating the change in absorbable photons in the enhanced region in each case (see the Supporting Information for details and further discussion), a clear linear relationship is observed outside of the saturated region (with cut-on wavelengths greater than or equal to 495 nm), which agrees well with other works (Figure 3e).[13b,26] The regression has a R^2 exceeding 0.99, including a fourth data point at the origin (no absorbed photons implies no threshold voltage shift). Thus, a clear relationship between the shift in threshold voltage and visible light absorption is revealed. This experiment excludes the possibility that the photodoping effect observed arises from excitation in either the CNT or oligomer alone. Rather the effect can only be explained by photoexcitation of the charge transfer complex formed between the two materials.

The solid-state absorption and field effect transistor photoresponse data suggest the formation of a charge transfer complex formed by the CNT and the oligomer. To determine the origin of this complex, the band alignment of the CNT and oligomer was examined. The Fermi level of the oligomer is assumed to lie at its intrinsic level (in the middle of its band gap because no dopant was present) while that of the CNT is assumed to reside at its valance band due to adsorbed oxygen (Figure 3f).[27] This alignment shows two key features. First, charge transfer occurring from the CNT to the LUMO of the oligomer must overcome an energy difference of 1.6 eV, which corresponds to a wavelength of 792 ± 89 nm. This agrees well with the solid-state absorption and FET photoresponse data. The other notable aspect is the formation of an electric field at the CNT/oligomer interface due to band alignment, in agreement

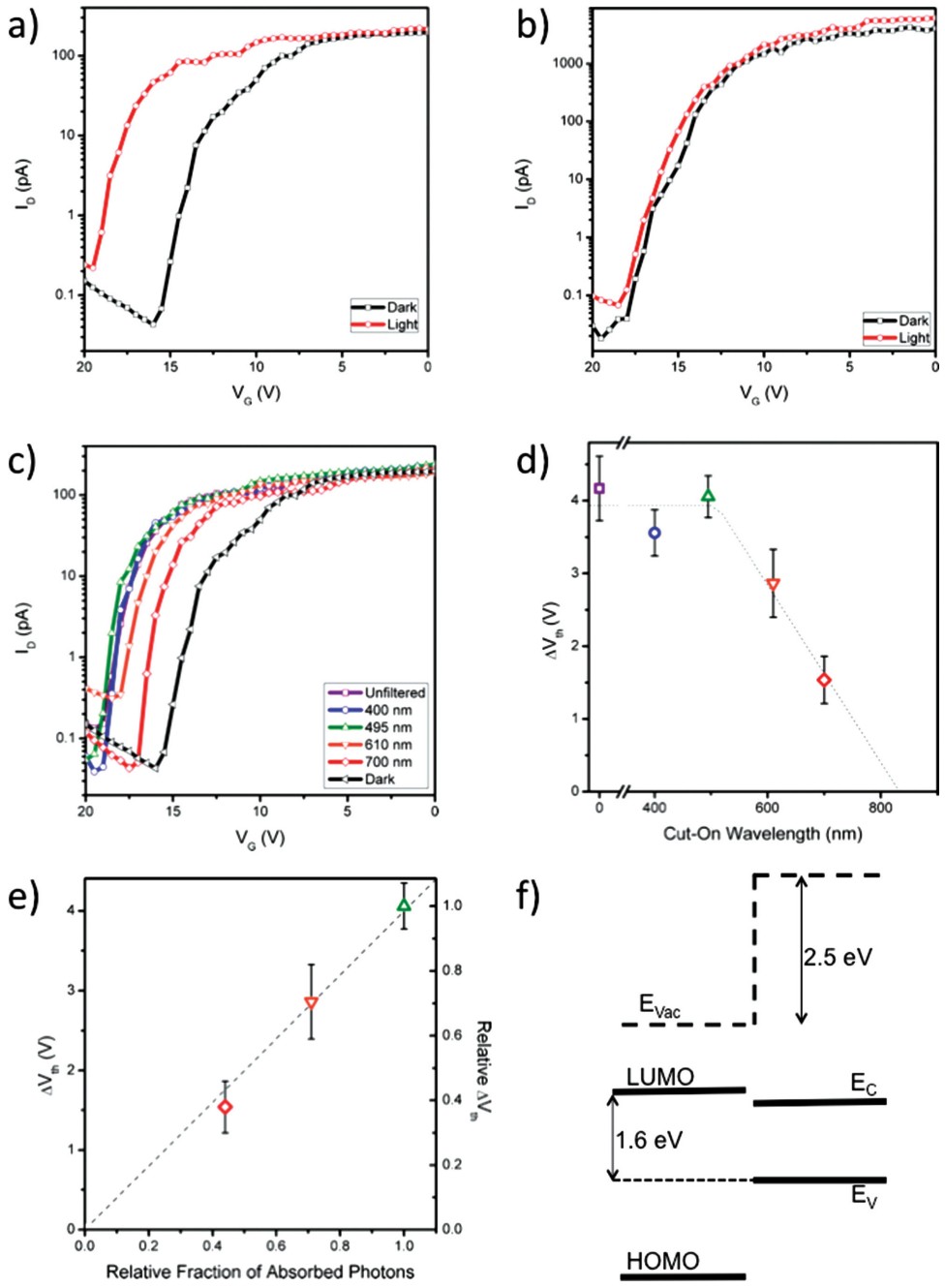

Figure 3. a) Transfer characteristics of the FETs fabricated using Tg-Car/CNT. Illumination with visible light causes a shift in threshold voltage. b) By contrast, no shift is observed in FETs fabricated using CNTs without the oligomer. c) Transfer characteristics obtained using long-pass filters with various cut-on wavelengths, keeping constant the flux of photons with energy exceeding the band gap of the CNT. d) The threshold voltage shift as a function of cut-on wavelength. As the fraction of photons with wavelengths below 833 ± 37 nm (1.5 ± 0.1 eV) decreases, the threshold voltage shift is reduced. Note that this does not correspond to the CNT's band gap, which excludes excitation in the CNT alone. e) Threshold voltage shift as a function of the relative number of photons that can be absorbed by the complex, featuring a linear correlation. f) Fermi level alignment between the oligomer and CNT suggests the formation of a charge transfer complex that corresponds to the enhanced absorption. Also noteworthy is an electric field created by a 2.5 eV energy barrier at the interface. This field might also hinder electron transfer back into the CNT, enabling the observed p-type doping.

with related work.[28] This field, with a potential of 2.5 eV, may enhance charge separation while preventing LUMO electrons from transferring back to the CNT from the oligomer. Essentially, the electric field directs electrons away from the CNT and toward the oligomer; it creates an energy barrier that an electron in the oligomer must overcome to transfer back to the CNT. Without significant back transfer, there is a net increase in hole population within the CNT. This is the proposed mechanism for the p-type photodoping observed. Furthermore, the Type I heterostructure traps holes in the CNT, which retains the

excess hole concentration. This suggests that the electric field also enhances charge separation, although further investigation is needed. The electric field might also play a role in the threshold voltage shift. For electrons to transfer into the CNT (which recombine with the holes, reducing the charge carrier density, and turning off the transistor), the built-in electric field must be overcome by the electric field generated by the gate electrode. Restated, the oligomer makes it more difficult to turn the transistor to the off state, leading to the increased threshold voltage. For more discussion on the energy level alignment, please see the Supporting Information.

It is worth noting that the majority CNT species are (6,5) and (7,6), which have E_{22} absorption peaks at 579 nm (2.2 eV) and 652 nm (1.9 eV), respectively, as extracted from the absorption data plotted in Figure 2b. These values are within the region of the enhanced absorption. However, E_{22} absorption can be eliminated as a cause of the photodoping. First of all, E_{22} absorption does not explain the broad increase observed in the absorption data (Figure 2). Secondly, the energetics are not favorable for photodoping. The E_{22} level in the conduction band lies very close to the LUMO of the oligomer. Although electron transfer from the CNT to the oligomer is still thermodynamically favorable, the dominant mechanism is likely thermalization to the E_{11} band as this process[29] is likely much faster than electron transfer.[30] Finally, a photoresponse was observed when using a cut-on wavelength of 700 nm, which eliminates E_{22} absorption in nearly all of the CNTs in the dispersion. Thus, the possibility of E_{22} absorption being the cause of the photodoping is excluded. Additionally, oxygen is known to affect threshold voltage under exposure to ultraviolet light. Although, virtually no ultraviolet light is present when using a tungsten lamp, Tg-Car/CNT transistors were tested in an argon environment and no oxygen-related effects were observed (Figures S7 and S8, Supporting Information).[31]

In summary, a Tg-Car/CNT complex was examined. The complex improved the optoelectronic performance of the CNTs in two ways. First, the oligomer dispersed the CNTs in chloroform and produced uniform, aggregate-free films on a SiO_2 surface, which represents an improvement in processability. Secondly, while the oligomer only absorbs ultraviolet light and the CNT has narrow absorption bands in the infrared band, the complex showed enhanced broadband absorption in the visible range through the formation of a charge transfer band. Field effect transistors fabricated using the Tg-Car/CNT material showed a p-type photodoping, which indicates that the oligomer acts as an electron acceptor in spite of its donor-like energy levels. It is proposed that energy level alignment between the oligomer and CNTs hindered the back transfer process, enabling a net increase in hole concentration in the CNTs. The results presented in this report may provide the basis for designing new dispersing molecules to extend the light absorption range of CNT/organic molecule composites and enhance charge separation. These aspects may be keys in realizing practical photovoltaic cells and photodetectors.

Experimental Section

Synthesis and Characterization of Carbazolylethynylene Oligomer: The carbazolylethynylene oligomers (Tg-Car) having triethylene glycol monomethyl ether (Tg) side chains were synthesized from the requisite 3,6-diiodocarbazole and 3,6-diethynylcarbazole using standard Sonogashira coupling conditions. The synthetic details can be found in ref.[22]. Gel permeation chromatography (GPC) analysis using polystyrene standards showed average masses of 6.4 and 11.4 kDa (for M_n and M_w, respectively), which correspond to a dispersity ($Đ$) of 1.8 and an average chain length of 19.

CNT Dispersion: To create the dispersion, 1.0 mg of CNTs (SWeNT SG 65, Southwest Nano Technologies) and 6.0 mg of Tg-Car were mixed in 9.0 mL of chloroform (reagent grade, Sigma-Aldrich or Fisher Scientific). The mixture was sonicated (Fisher Scientific FS30H Ultrasonic Cleaner) for 90 min. The suspension was centrifuged (IEC Centra CL2) at 4200 rpm (≈3000 g) for 20 min. A residue formed at the bottom of the tube. The suspension was removed and placed into a new tube. The centrifugation process was performed three times. Finally, the dispersion was centrifuged (Beckman Coulter, Microfuge 18) at a higher speed, 14 000 rpm (≈18 000 g) for 15 min; no residue was observed, indicating nearly complete dispersion of the CNTs.

Raman: Raman spectra measurements were performed on a Renishaw Raman microscope equipped with a 633 nm laser as the excitation source. The laser spot was adjusted to a domain of several microns. All Raman spectroscopy measurements were recorded in ambient conditions.

Atomic Force Microscopy: AFM samples were prepared by drop casting Tg-Car/CNT from a 5:1 dilution of the stock solution onto SiO_2 substrates, cleaned prior to deposition by sonication in acetone and isopropanol. After deposition, the samples were placed in chloroform and sonicated for 5 min to wash away the excess Tg-Car. Imaging was performed using a Veeco MultiMode V equipped with a high-resolution ("E") stage and a Veeco NanoScope V controller.

Absorption: Absorption spectra were obtained using an Agilent Cary 100 UV–vis spectrophotometer. Samples were prepared on quartz slides. In the case of the Tg-Car/CNT sample, the excess oligomer was rinsed away by drop casting chloroform and wicking the solvent with a swab. This process was repeated until no further change in the spectrum was observed.

Field Effect Transistor Fabrication: Field effect transistors were fabricated in the bottom gate, bottom contact configuration. Heavily doped (n-type) silicon wafers with a 300 nm thermal oxide layer were obtained from Silicon Quest (p/n 20020008), cleaned with acetone, isopropanol, and piranha, and patterned using a standard lithography procedure. Metallization was performed by sputtering 70 nm of Au with a Cr or Ti adhesion layer using a Denton Discovery 18 at 50 W and a base pressure of 2×10^{-6} torr. The electrode pairs featured 5 μm gaps with 100 μm widths. Substrates were cleaned again by sonication in acetone and isopropanol. Tg-Car/CNT was deposited from a 5:1 dilution of the stock solution by spin coating (500 rpm pre-spin for 9 s, followed by 30 s at 2000 rpm). Untreated CNTs were similarly deposited from a dimethylformamide suspension.

Field Effect Transistor Measurements: All measurements were performed under ambient conditions. Measurements were taken by an Agilent 4156C Semiconductor Analyzer with a Signatone probe station in a shielded dark box. The tungsten lamp intensity was set to 2.8 mW cm^{-2} for the unfiltered and 400 nm cut-on exposures. The settings were 2.7, 2.5, and 2.4 mW cm^{-2} for the 495, 610, and 700 nm cut-on exposures, respectively. Long-pass filters from Thor Labs were used to control the spectrum (FGL400, FGL495, FGL610, and FEL0700 for 400 nm, 495 nm, 610 nm, and 700 nm cut-on wavelengths, respectively). The lamp power settings were selected in order to hold constant the flux of photons with energies exceeding that of the CNT band gap. In every case, the drain-source voltage was −1 V. Threshold voltages were calculated by fitting the linear portion of the transfer curve.

Supporting Information

Supporting Information is available from the Wiley Online Library or from the author.

Acknowledgements

B.R.B. and M.X. contributed equally to this work. The authors would like to thank Z. Zhang for discussion and B. van Devener for his assistance with the adhesion force microscopy. Portions of this work were performed in the University of Utah's Nanofab and Micron Microscopy Core. B.B. and D.J. would like to acknowledge funding from the NSF IGERT (DGE0903715). Additionally, B.B. would like to acknowledge funding from the NASA Office of the Chief Technologist (NNX12AM67H) and the Wayne Brown Fellowship. This work was supported by funding from the NSF (CHE 0931466) and the Department of Homeland Security, Science and Technology Directorate (2009-ST-108-LR0005).

Received: September 5, 2014
Revised: October 9, 2014
Published online: November 4, 2014

[1] a) R. Saito, M. Fujita, G. Dresselhaus, M. S. Dresselhaus, *Appl. Phys. Lett.* **1992**, *60*, 2204; b) T. W. Odom, J.-L. Huang, P. Kim, C. M. Lieber, *Nature* **1998**, *391*, 62; c) J. W. G. Wildöer, L. C. Venema, A. G. Rinzler, R. E. Smalley, C. Dekker, *Nature* **1998**, *391*, 59.

[2] a) M. P. Ramuz, M. Vosgueritchian, P. Wei, C. Wang, Y. Gao, Y. Wu, Y. Chen, Z. Bao, *ACS Nano* **2012**, *6*, 10384; b) R. M. Jain, R. Howden, K. Tvrdy, S. Shimizu, A. J. Hilmer, T. P. McNicholas, K. K. Gleason, M. S. Strano, *Adv. Mater.* **2012**, *24*, 4436; c) X. C. Lau, Z. Wang, S. Mitra, *Appl. Phys. Lett.* **2013**, 243108.

[3] a) N. M. Gabor, Z. Zhong, K. Bosnick, J. Park, P. L. McEuen, *Science* **2009**, *325*, 1367; b) L. Yang, S. Wang, S. Zeng, Z. Zhang, T. Pei, Y. Li, L.-M. Peng, *Nat. Photon.* **2011**, *5*, 672; c) K.-H. Kim, D. Brunel, A. Gohier, L. Sacco, M. Châtelet, C.-S. Cojocaru, *Adv. Mater.* **2014**, *26*, 4363.

[4] a) T. Mueller, M. Kinoshita, M. Steiner, V. Perebeinos, A. A. Bol, D. B. Farmer, Ph. Avouris, *Nat. Nanotechnol.* **2010**, *5*, 27; b) Ph. Avouris, M. Freitag, V. Perebeinos, *Nat. Photon.* **2008**, *2*, 341.

[5] M. S. Dresselhaus, G. Dresselhaus, A. Jorio, *Annu. Rev. Mater. Res.* **2004**, *34*, 247.

[6] J. Chen, M. A. Hamon, H. Hu, Y. Chen, A. M. Rao, P. C. Eklund, R. C. Haddon, *Science* **1998**, *282*, 95.

[7] M. Holzinger, J. Abraham, P. Whelan, R. Graupner, L. Ley, F. Hennrich, M. Kappes, A. Hirsch, *J. Am. Chem. Soc.* **2003**, *125*, 8566.

[8] D. Tasis, N. Tagmatarchis, A. Bianco, M. Prato, *Chem. Rev.* **2006**, *106*, 1105.

[9] M. Zheng, A. Jagota, E. D. Semke, B. A. Diner, R. S. McLean, S. R. Lustig, R. E. Richardson, N. G. Tassi, *Nat. Mater.* **2003**, *2*, 338.

[10] L. S. Liyanage, H. Lee, N. Patil, S. Park, S. Mitra, Z. Bao, H.-S. P. Wong, *ACS Nano* **2012**, *6*, 451.

[11] A. Nish, J.-Y. Hwang, J. Doig, R. J. Nicholas, *Nat. Nanotechnol.* **2007**, *2*, 640.

[12] a) F. Wang, H. Gu, T. M. Swager, *J. Am. Chem. Soc.* **2008**, *130*, 5392; b) C. Y. Lee, R. Sharma, A. D. Radadia, R. I. Masel, M. S. Strano, *Agnew. Chem. Int. Ed.* **2008**, *47*, 5018.

[13] a) E. Kymakis, G. A. J. Amaratunga, *Appl. Phys. Lett.* **2002**, *80*, 112; b) S. Bhattacharyya, E. Kymakis, G. A. J. Amaratunga, *Chem. Mater.* **2004**, *16*, 4819; c) Y. Li, C.-K. Mai, H. Phan, X. Liu, T.-Q. Nguyen, G. C. Bazan, M. B. Chan-Park, *Adv. Mater.* **2014**, *26*, 4697.

[14] Z. Zhang, Y. Che, R. A. Smaldone, M. Xu, B. R. Bunes, J. S. Moore, L. Zang, *J. Am. Chem. Soc.* **2010**, *132*, 14113.

[15] a) Y. Che, H. Huang, M. Xu, C. Zhang, B. R. Bunes, X. Yang, L. Zang, *J. Am. Chem. Soc.* **2011**, *133*, 1087; b) H. Huang, C.-E. Chou, Y. Che, L. Li, C. Wang, X. Yang, Z. Peng, L. Zang, *J. Am. Chem. Soc.* **2013**, *135*, 16490; c) Y. Xia, P. Yang, Y. Sun, Y. Wu, B. Mayers, B. Gates, Y. Yin, F. Kim, H. Yan, *Adv. Mater.* **2003**, *15*, 353.

[16] a) M. Bernardi, M. Giulianini, J. C. Grossman, *ACS Nano* **2010**, *4*, 6599; b) H. Dai, *Acc. Chem. Res.* **2002**, *35*, 1035.

[17] C. J. Bender, *Chem. Soc. Rev.* **1986**, *15*, 475.

[18] a) K. Saito, V. Troiani, H. Qiu, N. Solladié, T. Sakata, H. Mori, M. Ohama, S. Fukuzumi, *J. Phys. Chem. C* **2007**, *111*, 1194; b) F. Cheng, J. Zhu, A. Adronov, *Chem. Mater.* **2011**, *23*, 3188.

[19] F. Lemasson, N. Berton, J. Tittmann, F. Hennrich, M. M. Kappes, M. Mayor, *Macromolecules* **2012**, *45*, 713.

[20] a) F. Lemasson, J. Tittmann, F. Hennrich, N. Stürzl, S. Malik, M. M. Kappes, M. Mayor, *Chem. Commun.* **2011**, *47*, 7428; b) N. Berton, F. Lemasson, F. Hennrich, M. M. Kappes, M. Mayor, *Chem. Commun.* **2012**, *48*, 2516.

[21] Y. Kanai, J. C. Grossman, *Nano Lett.* **2008**, *8*, 908.

[22] D. E. Gross, J. S. Moore, *Macromolecules* **2011**, *44*, 3685.

[23] S. Nanot, E. H. Hároz, J.-H. Kim, R. H. Huage, J. Kono, *Adv. Mater.* **2012**, *24*, 4977.

[24] C. Klinke, J. Chen, A. Afzali, Ph. Avouris, *Nano Lett.* **2005**, *5*, 555.

[25] R. B. Weisman, S. M. Bachilo, *Nano Lett.* **2003**, *3*, 1235.

[26] a) R. Martel, T. Schmidt, H. R. Shea, T. Hertel, Ph. Avouris, *Appl. Phys. Lett.* **1998**, *73*, 2447; b) D. S. Hecht, R. J. Ramirez, M. Briman, E. Artukovic, K. S. Chichak, J. F. Stoddart, G. Grüner, *Nano Lett.* **2006**, *6*, 2031.

[27] S.-H. Jhi, S. G. Louie, M. L. Cohen, *Phys. Rev. Lett.* **2000**, *85*, 1710.

[28] a) M.-H. Ham, G. L. C. Paulus, C. Y. Lee, C. Song, K. Kalantar-zadeh, W. Choi, J.-H. Han, M. S. Strano, *ACS Nano* **2010**, *4*, 6251; b) N. M. Dissanayake, Z. Zhong, *Nano Lett.* **2011**, *11*, 286; c) F. Lan, G. Li, *Nano Lett.* **2013**, *13*, 2086.

[29] C. Manzoni, A. Gambetta, E. Menna, M. Meneghetti, G. Lanzani, G. Cerullo, *Phys. Rev. Lett.* **2005**, *94*, 207401.

[30] S. D. Stranks, C. Weisspfennig, P. Parkinson, M. B. Johnston, L. M. Herz, R. J. Nicholas, *Nano Lett.* **2011**, *11*, 66.

[31] M. Shim, J. H. Back, T. Ozel, K. W. Kwon, *Phys. Rev. B* **2005**, *71*, 205411.